
Article:
Burns, Annika Lynn, Pickering, Matt, Green, Kimberley Ann et al. (5 more authors) (2017) Micromorphological and chemical investigation of late-Viking age grave fills at Hofstaðir, Iceland. Geoderma. pp. 183-194. ISSN: 0016-7061

https://doi.org/10.1016/j.geoderma.2017.06.021

Micromorphological and Chemical Investigation of late-Viking Age Grave Fills at Hofstaðir, Iceland

Annika Burns[a], Matthew D. Pickering[b], Kimberley A. Green[b], Adam P. Pinder[b], Hildur Gestsdóttir[c], Maria-Raimonda Usai*[a,d], Don R. Brothwell[a,1]†and Brendan J. Keely[b]

[a]Department of Archaeology, King's Manor, University of York, York, YO1 7EP, UK

[b]Department of Chemistry, University of York, Heslington, York, YO10 5DD, UK

[c]Institute of Archaeology, Bárugata 3, 101 Reykjavík, Iceland.

[d] Dipartimento di Architettura, Design, Urbanistica, Università degli Studi di Sassari, Palazzo del Pou Salit, Piazza Duomo (Via Manno) 6, 07041 Alghero (SS), Italia

*Corresponding author Maria-Raimonda Usai: Tel: 0039 3200481932 or 0039070273066,

E-mail address: mariaraimonda.usai@gmail.com

Highlights

- Complex relationships occur between inhumed human remains and their grave fills
- Weathering of volcanic silicates in grave fills can be affected by the human remains
- Point counting can effectively assess volcanic silicate weathering in grave fills
- Organic chemical signatures provide evidence for the former presence of a coffin
- Non-native wood indicates either foreign lumber import or driftwood utilization

[1]† Deceased on 26 September 2016

Abstract

Grave fills from seven human burials from a late-Viking age - early medieval cemetery at Hofstaðir, Mývatnssveit (Iceland) were examined by soil micromorphology and organic chemical analysis. Detailed analysis of the weathering of the mineral constituents of the grave fills demonstrates a relationship between the extent of weathering of volcanic silicates within the fills and the presence of buried human remains. Gas chromatography-mass spectrometry (GC-MS) of extracts from the fills and controls of two graves revealed organic signatures dominated by plant-derived organic matter, with no evidence of degradation products of the body tissues. Transformation of *n*-alkanes into *n*-alkan-2-ones provides evidence for microbial activity within the fills. GC-MS analysis of the organic extract from under one of the skulls and pyrolysis gas chromatography of wood fragments found in that grave provide compelling evidence for the former presence of a conifer wood coffin. The use of this non-native wood in the burial provides evidence for either the import of foreign lumber or the utilisation of driftwood, most likely originating from Russia/Siberia.

Keywords

Weathering; grave fills; human burials; micromorphology; post-depositional processes; tephra; organic residues; abietane and pimarane diterpenoids; coffin wood.

1. Introduction

Once deposited in soils, anthropogenic artefacts become part of an inter-dependent sedimentological, pedogenic and biological environment. Over the duration of their contact with the soil environment, such artefacts are subjected to suites of post-depositional processes that ultimately result in their total destruction or preservation, in varying states, as archaeological remains. The factors controlling the degradation pathways are in constant flux, determined by the dynamics of the archaeological environment (Schiffer, 1987).

Comprehensive archaeological interpretation of burials demands knowledge of the original nature and composition of buried remains and of the changes that have occurred over time. The InterArChive project aims to provide information on archaeological burials through micromorphological and organic chemical

analysis of the adjacent soils and sediments and thereby reveals both signatures imparted to the fills and impacts on the soils themselves (Usai et al., 2014). For example, interactions between degrader organisms consuming organic materials and the mineral components within a burial soil assemblage can leave traces within the soil including alterations to minerals (Huang, 2011; Mikuláš, 2008) while informative chemical signatures pertinent to the archaeological investigation of human burials can be preserved in the burial matrix associated with the remains (Pickering et al., 2014).

Once buried, carbon-based materials can be acted upon by heterotrophic organisms, including fauna, fungi and aerobic and anaerobic bacteria. These, in turn, generate new/or modified inputs to the soil system comprising secondary products and/or structures (Carter and Tibbett, 2008). Experimental research has been invaluable in interpreting the extent and nature of the preservation of artefacts as evidence of biotic processing (Bell et al., 1996; Crowther et al., 1996) and in understanding the effects of pedogenic processes over time (Canti, 2003). For decades, soil scientists have relied heavily on micromorphology to discern soil characteristics and their temporal, spatial and causal relationships (Brewer, 1964; Cornwall, 1958; Kubiena, 1938). The technique reveals the displacement and movement of materials and organisms through micro-contextual relationships, and has been implemented successfully in assessing stratigraphic integrity and in studies concerning site formation processes (Matthews et al., 1997). Together with complementary techniques, micromorphology can enable effective testing of the suitability of sampling strategies and analytical methodologies for isolating processes and agents in the degradation of materials (Courty et al., 1994; Macphail and Cruise, 2001). Integration of micromorphology with point counting has enabled interpretation of past pedological processes and concerned measurement of voids and porosity (Bouma et al., 1979; Jongerius, 1974; Jongerius et al., 1972; Marcelino et al., 2007; Pagliai, 2008; Stoops, 2010), clay coatings and infillings (Grossman, 1964), occurrence of micro-charcoal (Bennett et al., 1990) and deposits of illuvial clay (Eswaran, 1968; Murphy and Kemp, 1984). Here we assess the extent to which degraded organic materials can be identified through proxy evidence derived from micromorphological investigations complemented by organic analysis.

1.1. *Site introduction: Hofstaðir, Iceland*

Hofstaðir is an archaeological site in the district of Mývatnssveit, NE Iceland (64.23 / −19.64, < 50 m OD; Fig. 1), where archaeological investigations have been ongoing since the early 1990s. The graves and fills investigated were sampled by the InterArChive project team during an excavation held in 2011 by the Institute of Archaeology, Iceland (see Isaksen and Gestsdòttir, 2012 and Fig. 2)

Fig. 1: Landscape surrounding the site of Hofstaðir (blank square, see Fig. 2), Iceland with inset (images adapted from Google Maps © 2013). [Grayscale image provided]

The archaeological investigations at Hofstaðir have focused on two separate parts of the site, a Viking feasting hall dated to the late 10th early 11th century, the excavation of which was completed in 2002 (Lucas 2009), and the late Viking age – early medieval cemetery, situated 50 m south of the Viking age longhouse, where investigations were ongoing at the time of sampling (Gestsdóttir, 2015). The excavation of the cemetery started in 1999, and has to date revealed the presence of a circular boundary, c. 30 m in diameter, with a small central stave church, of which there are at least two construction phases. The burials, all inhumations, some in wooden coffins, surround the church. To date 134 graves have been excavated at the site. There is evidence of some internal organisation within the cemetery, with most of the women in the northern part, the men mostly in the southern part, and the children, in particular the neonates, up against the eastern wall of the church (Gestsdóttir, 2015). This organisation is commonly seen in cemeteries of this period, both in Iceland and elsewhere in northern Europe (Vésteinsson and

Gestsdóttir, 2011). It is not possible to exclude that other factors determined where within the cemetery an individual was buried. Recent palaeopathological analysis of osteoarthritis within the Hofstaðir skeletal collection has demonstrated that the people buried within the cemetery were to a large extent biologically related to each other (Gestsdóttir, 2014), although isotopic analysis has shown that there are individuals within the group who lived a significant proportion of their lives in a coastal area, suggesting that they were not native to the Mývatn region (Sayle et al. 2016). Dating of the cemetery has been based on tephrochronology and radiocarbon dating of human skeletal remains as well as birch from the earliest church structure. The construction of the cemetery boundary as well as the earliest burials occurs shortly after the *c.* AD940 eruption in Veiðivötn, and the burials in the cemetery all predate the AD1300 eruption in Hekla, and most likely burials ceased well before that, the early 12th century at the latest, based on radiocarbon dates. It is, however, likely that the church was in use longer (Isaksen and Gestsdóttir, 2012, Sayle et al., 2014, Gestsdóttir, 2015).

The soils of Iceland, referred to as andosols (IUSS, 2006), are developed from basaltic to andesitic volcanic materials. Although young, they display evidence of erosion and transportation processes. Basaltic volcanic glass, by contrast with more silica-rich materials, may be readily altered, leading to the production of palagonite and eventually allophane, imogolite and ferrihydrite (Arnalds and Oskarsson, 2007).

2. Materials and methods

2.1 Excavation

The seven graves (HSM-A-114 to 120) sampled for the InterArChive project in 2011 were all located within the northernmost part of the cemetery (Isaksen and Gestsdóttir, 2012; Fig. 2b). A comprehensive set of samples was collected, comprising 150 for organic chemical analysis and 26 for micromorphology. A local soil profile (C1) in undisturbed ground nearby was dug to act as a source of multiple controls (Figs. 2b and 3a). The samples from the seven graves were studied by comparison with the control profile (C1).

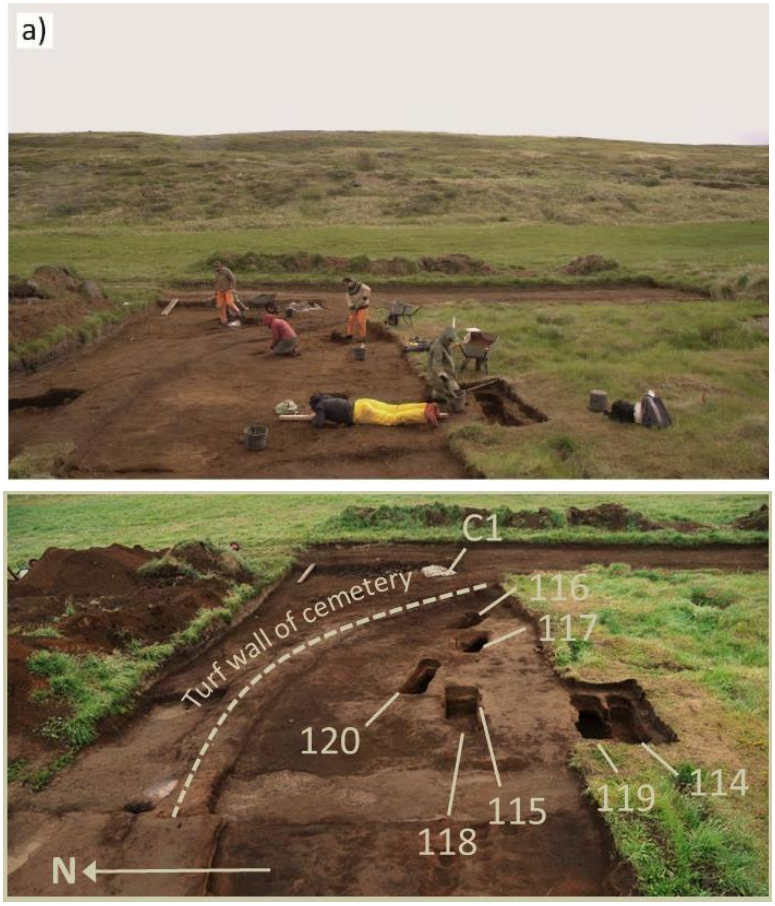

Fig. 2: a) Portion of site excavated in 2011 and b) location of the graves and C1 control profile within the cemetery at Hofstaðir, surrounded by turf walls. [Grayscale image provided]

Five of the seven graves sampled were undisturbed burials, containing complete and articulated skeletons. Graves HSM-A-115 and 118 were reburials, HSM-A-115 containing the remains of at least two individuals. The seven graves appeared, during excavation, to present variations in the levels of preservation, both in terms of completeness of the skeletal remains and in the physical condition of the bones. A sample of the fill near the sternum (Sample 15) within HSM-A-120 was reported by the excavators to contain ash, and the left femur of HSM-A-117 was heavily degraded and soft. Graves HSM-A-114, 116, 117 and 119 were all fairly complete in the skeletal remains whereas HSM-A-120 was moderately complete, and HSM-A-115 and 118 both represented charnel deposits.

2.2. Sampling

Samples of the burial matrix were collected from key anatomical locations on the skeleton according to the InterArChive sampling strategy (Usai et al., 2014) (locations and numbers detailed in Fig. 3, Table 1). A

minimum of 17 locations were targeted for chemical analysis and 4 key areas; head (1), pelvis (2) and feet (3/4) were targeted for micromorphological analysis. In some cases, however, the configuration of the skeletal remains precluded sample collection for some locations.

Site controls were collected from a profile (C1) through non-grave soil from the site. On site, the grave fill was interpreted as backfill, comprising material excavated during the digging of the grave. Two controls, C2 and C3, were collected from the grave fill as essential comparators of grave fill that has not been in contact with the buried remains (Fig. 3).

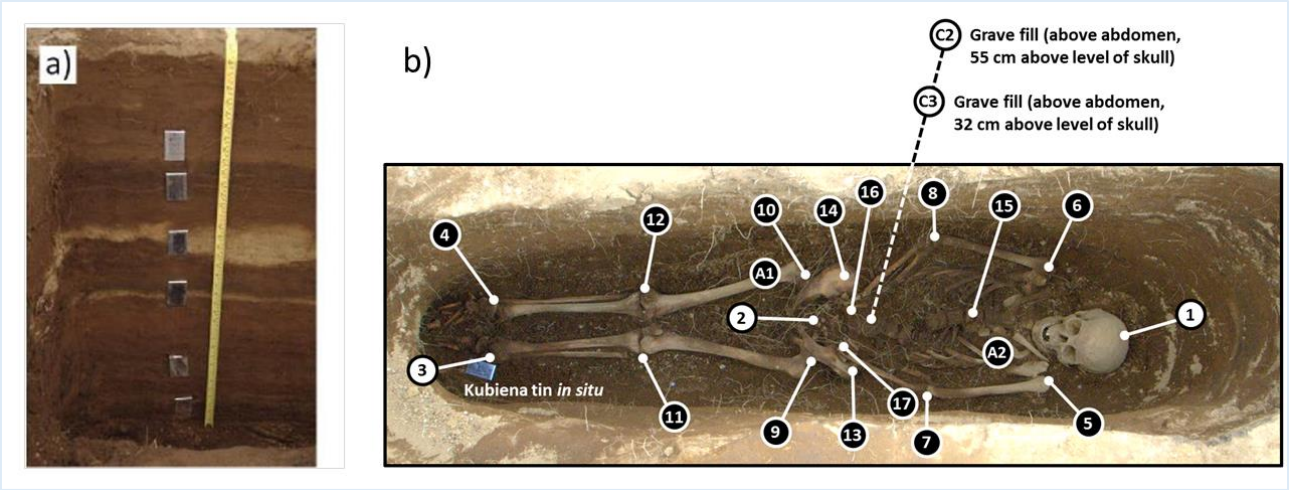

Fig. 3: Sampling locations at Hofstaðir for a), C1 non-grave soil and b), HSM-A-119 showing C2 and C3 controls and soil sample locations in the coronal plane of the skeletal remains. Black numbers against a white background indicate that fill was collected for both micromorphological and chemical analysis. White numbers against a black background indicate samples collected for chemical analysis only. Samples collected in addition to the prescribed sampling positions are prefixed with A. For a full sample list see Table 1. [Grayscale image provided]

Further to the prescribed sampling locations, additional samples (prefixed by the letter 'A') were collected in response to specific features of the individual graves. Grave fill samples for chemical analysis were collected proximal to the skeletal remains (designated x for above, y for adjacent and z for below) using a spatula, wrapped in pre-cleaned foil, placed in geochemical sample bags and stored cold. On return to the laboratory, samples were stored frozen until required for analysis. Grave fill samples for micromorphology were collected from undisturbed archaeological sediment or grave fills using Kubiena tins (83 × 50 × 32 mm,

83 × 55 × 42 mm, and 65 × 38 × 28 mm).

Table 1. Samples collected for organic chemical analysis. The location of the sample in the coronal plane of the skeletal remains is indicated by the sample number (Fig. 3b) whereas the vertical location of the sample (i.e. just above, adjacent to or just below the bone) is indicated by suffix x, y or z. Suffixes A and B denote samples collected in addition to the defined positions.

Grave	Sample number	Description
HSM-A-116	C2	Control above abdomen (7 cm depth, 66 cm above level of skull)
	C3A	Control above skull (36 cm depth, 37 cm above level of skull)
	C3B	Control above abdomen (36 cm depth, 37 cm above level of skull)
	1y and 1z	Skull (adjacent and below)
	2y and 2z	Pelvis (adjacent and below)
	3y and 3z	Left foot (adjacent and below)
	4y and 4z	Right foot (adjacent and below)
	5y and 5z	Left shoulder (adjacent and below)
	6y and 6z	Right shoulder (adjacent and below)
	7y	Left elbow (adjacent)
	8y	Right elbow (adjacent)
	9z	Left hip (below)
	10z	Right hip (below)
	11z	Left knee (below)
	2y and 12z	Right knee (adjacent and below)
	13y and 13z	Left iliac (adjacent and below)
	14y	Right iliac (adjacent)
	15x	Chest (above)
	16z	Right hand (below)
	17z	Left hand (below)
	A1	Black/brown stain above mandible
	A2	Possible coffin stain above thighs
	A3	Sample of wood above thighs
	A4	Sample of wood next to right hip
	A5	Beneath ribs on right hand side
	A6	Beneath lumbar vertebrae
	A7	Base of grave below shoulders
	A8	Base of grave below sample 10
	A9	Base of grave below sample 12
HSM-A-119	C2	Control above abdomen (15 cm depth, 55 cm above level of skull)
	C3	Control above abdomen (38 cm depth, 32 cm above level of skull)
	1y and 1z	Skull (adjacent and below)
	2x, 2y and 2z	Pelvis (above, adjacent and below)
	3y	Left foot (adjacent)
	4y	Right foot (adjacent)
	5y	Left shoulder (adjacent)
	6y	Right shoulder (adjacent)
	7	Left elbow
	8	Right elbow
	9y	Left hip (adjacent)
	10y	Right hip (adjacent)
	11z A and B	Left knee (below)
	12z	Right knee (below)
	13z A and B	Left iliac (below)
	14z A and B	Right iliac (below)
	15y and 15z	Collected as one
	16z	Right hand (below)
	17z	Left hand (below)
	A1	Dark deposit above top of femur
	A2	Under left scapula

2.3. Analysis of macroscopic organic remains

A single small sample from the pelvic area of grave HSM-A-114 was examined for its macrofossil remains. The sediment was weighed and left to soak in with water for a few days before being sieved to 0.3 mm. All fractions of the residue from sieving were examined in water, using low-power microscopy (× 50).

2.4. Manufacture of thin sections

The samples were dried in the tins through acetone vapour exchange (Miedema et al., 1974) and impregnated under vacuum with a slow curing polyester resin (Polylite 32320-00). The resulting consolidated soil blocks from the controls (C1, C2, and C3) were cut to produce one thin section from each, whilst samples from the fills adjacent to the skeletal remains (Samples 1, 2, or 3) were each cut to produce two thin sections: one tangential and one perpendicular to the body. The cut sections were back-polished, mounted, cut and ground to 30 μm thickness, with final 3 μm and 1 μm polishes.

2.5. Optical microscopy

Micromorphological observations were performed using a petrographic microscope (Zeiss AxioLab A1) equipped with a Zeiss AxioCamERc5s camera and AxioVision imaging software. Micromorphological descriptions were carried out employing the terminology of Stoops (2003) except for the relationship between the coarse and fine fraction, which was described with the terminology of Courty *et al*. (1989). The concepts of Delvigne (1998) were employed to describe mineral alteration, as this treatise includes concepts for alteration of a wide variety of mineral species, suited to the objectives of this investigation.

Point counting was performed under both parallel and cross polarized light at ×100 magnification using an AxioScope A1 microscope with motorized stage and equipped with an AxioCamMRc camera. More than 1000 counts were performed for each tangential and control thin section. Perpendicular sections were analysed in vertical sub-divisions, at 0.5 cm increments of distance from the skeletal remains, with a minimum of 500 counts per sub-division. Values for the organic materials were recorded as estimated mean abundance using abundance charts of Stoops (2003)). Tephra weathering ratios were calculated for each area sampled (thin section or sub-division). The degree of mineral weathering was established on the basis of the concepts of Delvigne (1998) and related to the percentage volume of grains which, through

weathering, had changed from their primary state to either a secondary product or a void. Tephra weathering was determined on the basis of mineralogical alterations revealed through changes in colour, opacity, internal void space, shape, fractures and internal structure. The degree of weathering was classified during point counting into extents 0-4 as follows: extent 0 (0-2.5% altered), extent 1 (2.5-25% altered), extent 2 (25-75% altered), extent 3 (75-97.5% altered), extent 4 (>97.5% altered) (Delvigne et al., 1979; Delvigne, 1998). The weathering ratio was calculated as a ratio of relative amounts of the heavily weathered (extents 3 + 4) to less weathered (extents 0 + 1 + 2) tephra. Hence higher values of the ratio reflected more heavily weathered tephra.

2.6 Scanning electron microscopy

Sub samples for SEM were cleaned and dried. The material was cut with razor blades, mounted on aluminium stubs using epoxy resin and earthed using Acheson Silver DAG glue. A layer of gold/palladium (7 nm) was applied to the mounted samples using a sputter coater. Images from the freshly cut surface were obtained under vacuum using a JEOL JSM-6490LV scanning electron microscope.

2.7. Organic chemical analysis

2.7.1. Sample preparation and solvent extraction

All solvents used were analytical grade or higher. All glassware was baked (450°C, 6h) prior to use using a Pyroclean Trace oven (Barnstead International, USA) to remove organic contaminants. Frozen samples were freeze dried using a HETO PowerDry PL3000 (Thermo, Hemel Hempstead, UK). Dry samples were disaggregated with a pestle and mortar, and sieved using 1 mm, 400 µm and 200 µm sieves. All subsequent work was performed on the sub 200 µm fraction. Extraction was performed using an accelerated solvent extraction system (ASE 350, Dionex, Hemel Hempstead, UK). Prior to loading samples, the empty extraction cells were subjected to extraction using the same solvents and conditions as for the samples. Soil (3-6 g) was loaded into 5 ml stainless steel cells and extracted three times with dichloromethane:methanol (9:1 v/v; 5 min at 100°C and 1500 psi). A blank extraction was also performed to assess whether any contamination was being introduced at the extraction step. Solvent was removed using a rotary vacuum concentrator (RVC 2-25, Christ, Osterode am Harz, DE). The total extract was divided into two portions, one of which was fractionated using a custom made glass chromatography column (90

mm × 10 mm i.d.) packed with silica gel (750 mg, height in column = 20 mm). The column was conditioned by washing with three bed volumes each of dichloromethane:methanol (1:1, v/v) and dichloromethane followed by equilibration with hexane. The extract to be fractionated was dissolved in dichoromethane (200 µl), spiked onto silica gel (40 mg) and the solvent removed in vacuo. The impregnated silica was loaded onto the top of the packed chromatography column. The column was washed with three bed volumes each of i) hexane, ii) hexane:toluene (1:1, v/v), iii) hexane:ethyl acetate (4:1, v/v) and iv) dichloromethane:methanol (1:1, v/v) to generate four chromatographic fractions: i) aliphatic hydrocarbons, ii) aromatic hydrocarbons iii) alcohols and esters and iv) acids, respectively. Solvent was removed using a rotary vacuum concentrator.

2.7.2. Derivatisation

Total extracts and polar (iii and iv) fractions were reconstituted in dichloromethane:methanol (2:1, v/v; 300 µl) followed by addition of trimethylsilyl diazomethane (20 µl) and allowed to react for 30 min, before drying under a gentle stream of nitrogen gas. Immediately prior to analysis, total extracts and polar fractions were heated with *N,O*-bis(trimethylsilyl)trifluoroacetamide (100 µl, containing 1% trimethylchlorosilane) and 5 drops of pyridine for 1.5 h at 60°C before reducing to dryness under a gentle stream of nitrogen gas.

2.7.3. Elemental Analysis (EA)

Carbon, hydrogen, nitrogen, sulfur, oxygen (CHNS-O) and total organic carbon (TOC) elemental analysis was performed using a Flash 2000 elemental analyser (Thermo, Hemel Hempstead, UK) fitted with a MAS200R autosampler, chromatographic column and thermal conductivity detector. Helium was used as a carrier gas at a flow rate of 140 ml min^{-1}. Sediment samples (10-15 mg) were weighed using a XS3DU microbalance (Mettler Toledo, Leicester, UK) into tin or silver foil capsules for CHNS or TOC analysis, respectively. Sediment samples for TOC analysis were treated with 2 drops of hydrochloric acid (6 M) to destroy carbonates before heating to 80°C for 6 min to drive of excess acid solution. Foil capsules were folded to exclude air. Samples were combusted in a quartz reactor tube packed with copper oxide granules and electrolytic copper wires and held at 900°C. Sample introduction coincided with a pulse of oxygen (250 ml min^{-1}, 5 s). For oxygen analysis, sediment samples (10-15 mg) were weighed into silver foil capsules and

folded to exclude air. Thermal decomposition of the sample was achieved in a quartz reactor tube, packed with nickel plated carbon and quartz turnings and held at 1060°C. Carbon dioxide and moisture was removed from the reactor stream by passage through an absorption filter containing granules of soda lime and magnesium perchlorate. Instrument control, data acquisition and processing was by Eager Xperience V1.11 (Thermo, Hemel Hempstead, UK).

2.7.4. Gas chromatography (GC) and gas chromatography-mass spectrometry (GC-MS)

Total lipid extracts were analysed using a Trace GC Ultra gas chromatograph (Thermo, Hemel Hempstead, UK) equipped with a Triplus autosampler, a fused silica capillary column (J&W DB-5, 60 m × 0.32 mm i.d., 0.25 µm film thickness, Agilent, Wokingham, UK) and a flame ionisation detector (FID). Samples were prepared in dichloromethane and volumes of 1 µl injected onto the column via a splitless injection port (280°C, split flow 1:25, splitless time 0.8 min). The oven temperature was programmed from an initial temperature of 70°C to 130°C at a rate of 20°C min^{-1} and then to 320°C at a rate of 4°C min^{-1} where it was held for 40 min. Helium was used as a carrier gas at a flow rate of 2 ml min^{-1}. The FID was held at 330°C. Instrument control, data acquisition and analysis was by ChromQuest 5.0 V3.2.1 (Thermo, Hemel Hempstead, UK).

Chromatographic fractions (i-iv) were analysed using an identical gas chromatograph to that above equipped with an ultrafast column module (UFC-5, 10 m × 0.1 mm i.d. 0.1 µm film thickness, Thermo, Hemel Hempstead, UK). Samples were prepared in dichloromethane for analysis and volumes of 1 µl injected onto the column via a split injection port (280°C, split flow 1:100) and the FID held at 330°C. The column oven was programmed from an initial temperature of 50°C (0.5 min isothermal) to 330°C at a rate of 90°C min^{-1} where it was held for 4 min. Helium was used as the carrier gas at a flow rate of 0.5 ml min^{-1}.

GC-MS analysis was performed on selected fractions using a 7860A gas chromatograph (Agilent, Wokingham, UK) equipped with a 7683B Series autosampler coupled to a GCT Premier Micromass time of flight mass spectrometer (Waters, Elstree, UK). Separation was achieved on a fused silica capillary column (Zebron, ZB-5, 30 m × 0.25 mm i.d., 0.25 µm film thickness Phenomenex, Macclesfield, UK). Samples were prepared in dichloromethane for analysis and volumes of 1 µl injected onto the column via a split injection

port (280°C, split flow 1:5). The oven was programmed from an initial temperature of 70°C to 130°C at a rate of 20°C min^{-1} and then to 320°C at a rate of 4°C min^{-1} where it was held for 40 min. Helium was used as the carrier gas at a flow of 1 ml min^{-1} and the MS transfer line set to 300°C. Mass spectra were acquired over the range 50-750 *m/z* units (cycle time 0.2 s) using an electron ionisation energy of 70 eV. Instrument control, data acquisition and processing was by MassLynx V4.1 (Waters, Elstree, UK). Compounds were identified from interpretation of their mass spectra and comparison with library spectra (NIST 08) where available.

2.7.5. Pyrolysis-gas chromatography (Py-GC)

Pulverised samples were analysed by pyrolysis-gas chromatography using a CDS Pyroprobe 5150 (Chemical Data Systems) interfaced with a Thermo Trace GC Ultra gas chromatograph. Samples were loaded into quartz boats (pre-cleaned at 1000°C, 20 s) and placed into a resistively heated platinum coil probe. An initial thermal desorption step was performed (interface temp 290°C, 3 min) and the compounds evolved vented prior to pyrolysis in helium at 610°C (15 s; interface temp, valve oven and transfer line 310°C). The gaseous pyrolysate was admitted via a splitless inlet (310°C, split flow 1:25, splitless time 0.8 min) onto a fused silica capillary column (J&W DB-5, 60 m × 0.32 mm i.d., 0.25 µm film thickness). Oven temperature programme: 50°C (isothermal 5 min) to 320°C (20 min) at a rate of 4°C min^{-1}. Helium was used as a carrier gas at a flow rate of 2 ml min^{-1} and the FID detector was held at 330°C.

3. Results and discussion

The grave soils were examined to determine the extent to which signatures relating to the presence of the organic remains associated with the burial could be detected in the soils and distinguished from background organic matter in the controls. Two distinct type of controls were examined: a series of samples from the control soil profile C1 and grave fills C2 and C3 from above the level of the buried remains. The controls from the fills reflect the matrix in which the burial is contained and is presumed to comprise backfill of the material dug in the construction of the grave. As such, it provides the best available representation of the source of the soil that is now intimately associated with the buried remains.

3.1 Macroscopic organic remains in pelvic sample from HSM-A-114

The sample comprised dark reddish-brown, soft, unconsolidated sand-sized grains with a few <1 mm clasts of buff silt-sized grains and some modern roots. On disaggregation, it yielded a very small residue, *c.* 50 cm^3, of which a few cm^3 were modern roots. The sample also contained quite a few small (up to 15 mm) fragments of bone, mainly from fish, with traces of wood charcoal (up to 5 mm). There was a single very decayed beetle elytron fragment and quite a few structures thought to be sclerotia (resting bodies) of the soil-dwelling fungus *Cenococcum geophilum Fr.* and megaspores of the low-growing pteridophyte lesser clubmoss, *Selaginella selaginoides (L.).* Both were interpreted to be ancient and are associated mainly with topsoil. The reddish brown undisaggregated sediment, also observed in small clasts of material which had not completely dispersed, could perhaps relate to the presence of peat ash.

3.2 Thin section descriptions

In order to investigate the interaction between the buried human remains and silicic tephra material within the graves, fills surrounding skeletal remains in seven graves were examined using micromorphological analysis with well tested approaches (Stoops et al., 2010) augmented by point counting (Bennett et al. 1990; Marcelino et a., 2007). Micromorphological observations were made on the sediment's basic attributes and organic and inorganic inclusions (Table 2). The mineral compositions, pedofeatures and pedality of the control profile and the grave fills were analysed in thin section. Most samples displayed undifferentiated b-fabric, suggesting an original material rich in organic matter. Root remains were evident in most samples (recorded as plant remains in Table 2); channel- shaped voids can provide evidence of bioturbation by soil fauna and/or flora. Chamber shaped voids both in controls and grave fills provide evidence of soil fauna, whereas other pedofeatures related to soil micro-fauna, such as excrement, were rare. All -materials were apedal, suggesting a young soil. Coarse grains embedded within the fine material comprised silicate minerals, feldspars, olivine and pyroxenes, in both control and grave fills. Tephra fragments were assessed according to their size, vesicularity, colour composition (rhyolitic to basaltic and phenocrysts) and roundness (Table 2).

The extent and pattern of mineral weathering in the control and grave fills from Hofstaðir was assessed semi-quantitatively by point counting, on thin sections taken tangential to the skeletal remains (Section

2.5), using an extension of the system proposed by Delvigne (1998). Although concerns relating to the reproducibility of point counting results obtained by different operators have been expressed (McKeague et al., 1980; Murphy, 1983; Miedema, 2002), support for its application in this work comes from the comparability of results with those obtained using complex image analysis techniques, including use of principal component images (Terribile and Fitzpatrick, 1995), and its effectiveness (discerned as the confidence in the reliability of results) when employed systematically by a skilled operator (Murphy, 1983; Kuhn et al., 2010). Thus, mineralogical alterations were revealed through changes in colour, opacity, internal void space, shape, fractures and internal structure (see Section 2.5).

During point counting, features were classified into one of nine possible groups: relatively unweathered tephra, rock fragments and mineral (extent 0-1); partially weathered tephra (extent 2); highly weathered isotropic tephra alteromorph (extents 3 or 4); highly weathered anisotropic tephra alteromorph (extents 3 or 4); fine materials; voids; nodules and coatings; organic; and other (undefined features). Weathering of inorganic materials was computed from the ratio of low extents (0, 1, or 2) to high extents (3 or 4): higher ratio values reflect more extensive weathering. The ratios were calculated from the percentage values from point counting rather than the raw counts to achieve comparability over differing surface areas of thin sections. The tephra weathering ratio in the soil profile shows an increase in the intensity of weathering with depth (Table 3). Given the low levels of bioturbation in the control soils, the weathering can be ascribed to abiotic factors. Notably, even at the greatest depth in the control profile (51-56 cm), the weathering ratio was substantially less than in any of the tangential sections of grave fills (Table 3). Furthermore, distinctly lower weathering ratios were determined for the grave fill controls (C2 and C3) from above the levels of the burials then from samples adjacent to the skeletal remains (skull, pelvic and feet areas; Table 3 and Fig. 4).

Table 2: Micromorphological observations from analysis of thin sections from the control profile (C1) and grave HSM-A-114.

						Voids[6]				Inorganic					Organic			
TS[1]	Sample[2]	Micro units	c/f[3]	BF[4]	RD[5]	Vesicles	Channels	Chambers	Vughs	Feldspars	Pyroxenes	Olivine	Tephra	Other[7]	AOM[8]	Excrement	Plant	Other[9]
C1 Profile																		
715	a	a	25/75	U	E	*	**	*	***	**	*	*	***	**	-	-	*	*
741	bc	b	90/10	U	LC		**	*	***	-	-	-	*****	*	-	-	*	-
741	bc	c	15/85	U	E	*	***	**		**	*	*	***	-	-	-	*	**
620	de	d	20/80	U	E		**	***	*	*	-	*	**	***	-	-	*	*
620	de	e	90/10	SP	E	-	***	***		*	-	-	**	*****	-	-	*	-
623	fh	f & h	15/85	U	E	*	**	**	*	**	*	*	**	-	-	-	**	*
623	fh	g	5/95	SP	E	*	**	*	**	**	-	-	*	***	-	-	-	-
599	hj	j	25/75	U	E	*	*	***	*	**	**	*	***	-	-	-	**	*
Grave HSM-A-114																		
680	1t	1 of 2	20/80	U	E	**	**	***	**	***	*	-	***	-	**	-	**	**
680	1t	2 of 2	40/60	U	E	*	*	**	**	**	-	-	***	-	**	-	**	-
730	1p	1 of 2	25/75	U	E	*	***	***	*	*	-	*	**	-	*	-	***	**
734	1p	1of 2	20/80	U	E	-	***	*	***	*	-	-	**	-	-	-	*	*
734	1p	2 of 2	45/55	U	E	-	**	-	***	*	-	-	***	*	***	-	*	-
713	2p	1 of 2	25/75	SP	E	-	***	**	**	**	-	*	**	**	*	-	-	**
713	2p	2 of 2	20/80	U	E	*	**	***	**	**	-	-	***	*	**	-	***	***
729	3,4t	1 of 2	15/85	U	E	*	**	***	*	**	*	-	**	**	-	-	**	-
729	3,4t	2 of 2	30/70	U	E	-	**	**	***	*	-	*	***	**	-	-	*	*
843	3,4p	1 of 3	30/70	U	E	-	**	**	**	*	-	*	***	*	-	-	*	*
843	3,4p	2 of 3	55/45	SP	E	**	*	**	*	-	-	*	***	-	-	-	*	*
843	3,4p	3 of 3	20/80	U	LC	*	-	**	**		-	-	*****	****	-	-	-	*
726	16t	1 of 2	20/80	U	E	-	-	**	**	***	**	*	****	**	-	-	*	-
726	16t	2 of 2	30/70	U	E	-	***	*	****	*	*	*	***	*	*	**	**	-

[1] Thin section number.

[2] Thin section cut tangential to the skeletal remains, p section cut perpendicular to the skeletal remains.

[3] c/f (coarse to fine ratio at 50 µm limit).

[4] birefringence fabric (BF: U = undifferentiated; SP = speckled).

[5] related distribution (E = embedded, LC = linked and coated).

[6] only one thin section showed cracks, identified as post sampling feature. Symbols represent not observed (–), negligible (1-2%) (*), few (2-5%) (**), some (5-10%) (***), common (10-20%) (****), abundant (>20%) (*****).

[7] e.g. mica

[8] amorphous organic matter

[9] e.g. fungal spores

Table 3: Summary of weathering ratio of tephra from the C1 control profile and from graves HSM-A-114 to 120: intra-grave controls, C2 and C3, and tangential thin sections.

	C1 Profile	Control fill / sample number	Graves						
			HSM-A-114	HSM-A-115	HSM-A-116	HSM-A-117	HSM-A-118	HSM-A-119	HSM-A-120
Depth below surface / cm	**Weathering ratio**		**Weathering ratio**						
a; 13-19	0.13	**C2**	ns*	0.52	0.34	0.48	0.42	0.31	0.21
bc; 22-28	0.11								
de; 35-41	0.08	**C3**	0.31	0.35	0.39	0.44	0.30	0.43	0.54
fh; 59-55	0.11								
hj; 70-76	0.42								
		1a	0.64	1.32	0.57	0.89	ns	1.07	1.14
		2a	1.34	ns	1.67	0.83	ns	1.46	2.24
		3/4a	0.75	ns	1.38	1.18	ns	1.42	1.50

* no sample collected

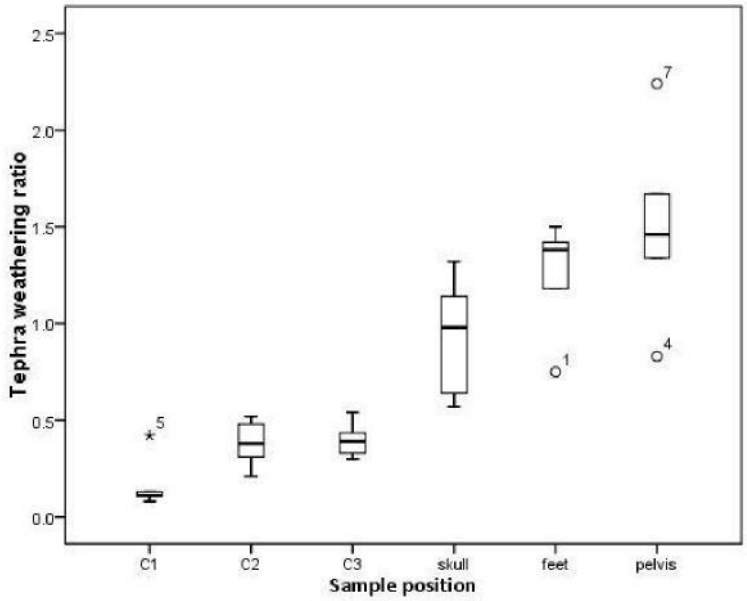

Fig. 4: Box and whisker diagram of the extent of tephra weathering within the tangential thin sections from Hofstaðir (at the 95% confidence level). Symbols (open circles and star) and their related numbers (5, 1, 7 and 4) represent outliers from the values shown in Table 3. Ratios increase (signifying an increase in the progression of the weathering of tephra) from the site controls (C1) to the intra-grave controls (C2 and C3) and the samples collected adjacent to the skeletal remains (skull, feet, and pelvis).

3.3. Thin section observations of biotic weathering processes

A distinct mode of alteration of tephra was observed through the presence of an isotropic phase with a dark grey colour in PPL (Fig. 5a). Support for this interpretation comes from similarities with the key optical characteristics of partially developed mineral alteromorphs at intermediate stages of weathering illustrated by Delvigne (Delvigne, 1998). The presence of plant- or fungal-derived organic matter in close association with altered mineral grains provides compelling evidence for the role of biota in the alteration (Fig. 5a and b). Fungal boring directly into tephra was evident from the presence of tracts, comprising holes and tubules, within tephra minerals, the fungal remains having been removed by decay processes (Fig. 5c and d). Fungal remains, including sclerotia, spores, and mycellae were observed both in the micromorphology thin sections and through bulk environmental analysis. The kingdom fungi includes endoliths, organisms that inhabit hard substrates (Tapanilla, 2008). In particular, some ectomycorrhizal and saprophytic fungal species are capable of boring into feldspar and quartz minerals. Typically, only *c.* 1% of the fungal micro-pores in minerals preserve the hyphae that formed them (Jongmans et al., 1997).

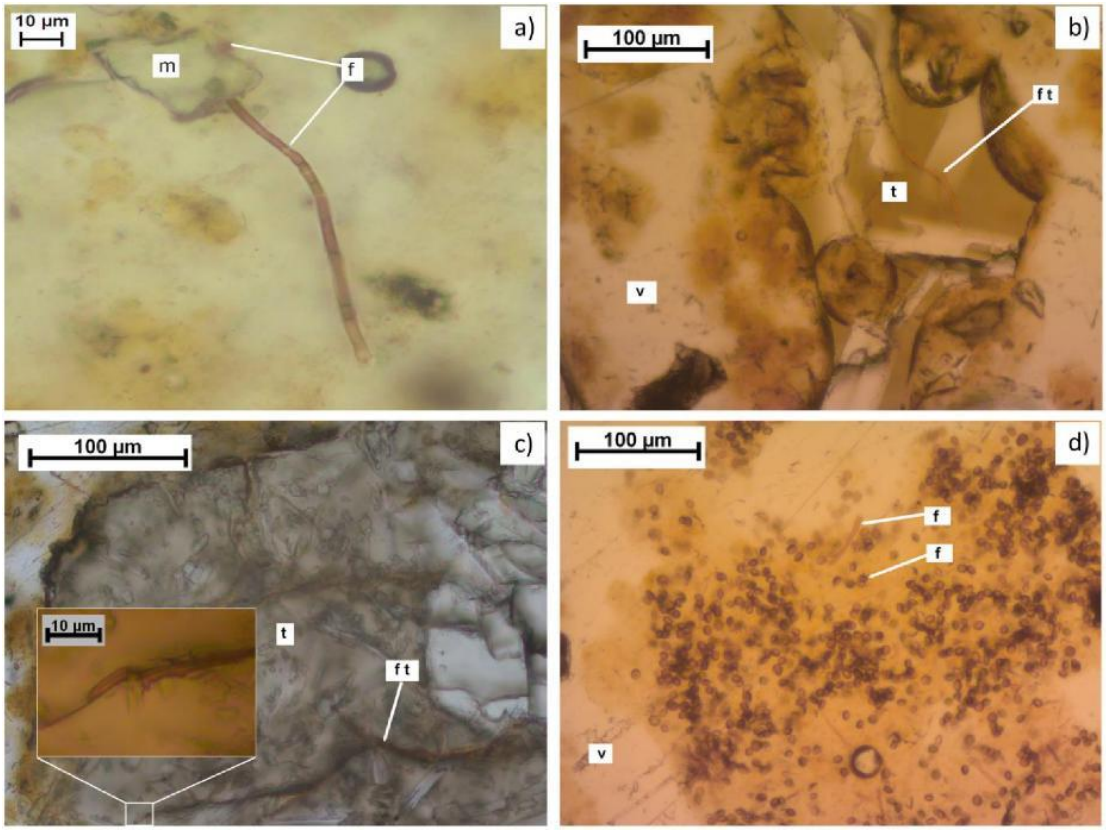

Fig. 5. Microscopy images from HSM-A-116 Sample 2 (PPL) a) weathered quartz mineral grain (m) in association with fungal remains (f); b) partially weathered tephra (t) displaying tract of fungal attack (f t) in association with a void (v); c) partially weathered tephra (t) displaying tract of fungal attack (f t) with inset showing detail at end of fungal tract; d) fungal spores (f) in association with a void (v) [grayscale image provided]

The combined mean surface area abundances of fungal remains from micromorphological observations of tangential and perpendicular thin sections from all controls and graves revealed distinct differences between the controls and the samples. The greatest levels of fungal remains were associated with samples adjacent to the skeletal remains (skull pelvis and feet), which also have high tephra weathering ratios (Fig. 6). Notably, samples from adjacent to the skeletal remains present evidence of greater fungal activity and tephra weathering than in the intra-grave controls (C2 and C3). The correlation of tephra weathering ratio and fungal remains (Fig. 6), combined with the evidence of fungal invasion of tephra (Fig. 5) and recognition of ancient fungal sclerotia in the pelvic sample examined for macroscopic organic remains (Section 3.1), suggests the two factors are linked. Microbial alteration of soil minerals was reported to be a significant

factor in mineral weathering patterns (McLoughlin et al., 2008) and it has been suggested that it may selectively solubilise elements despite the competing forces associated with surface charge (Bennett et al., 2001). Significantly, it was found here to result in deviations from a trend of increasing weathering with depth (Table 3; Figs. 4-6) whilst the fungal alteration parallels the weathering ratio (Fig. 6).

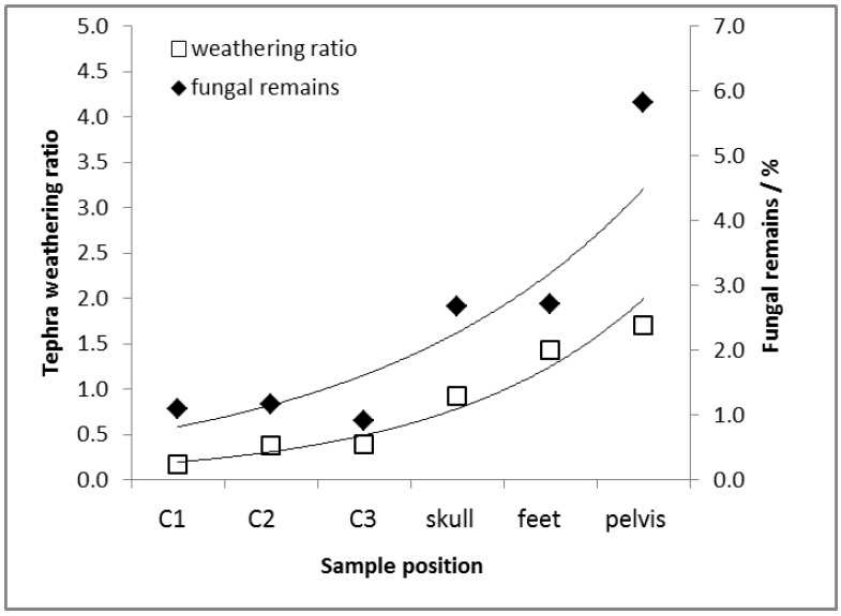

Fig. 6: Mean weathering ratio and abundance of evidence of fungal activity in all controls and grave fills from Hofstaðir. Exponential trendlines reveal the positive relationship between fungal presence and highly developed mineral alteromorphs. Mean weathering ratios represent >5000 counts for C1, >6000 for C2, >7000 for C3, >33,500 for skull, >24,500 for pelvis, and >21,500 for feet. Skeletal adjacent samples (skull, pelvis and feet) combine the results from both the tangential and the perpendicular thin sections.

The difference in weathering ratio between the control profile (C1) and intra-grave controls (C2 and C3) is interpreted as a product of disturbance associated with the cutting of the grave (Fig. 4). The evidence of an increase in tephra weathering with proximity to the human remains, and lower extent of weathering in the grave fills, C2 and C3, indicates a marked influence associated with the buried remains. Thus, the extent of tephra weathering was impacted significantly by the high organic matter content from the inhumation.

3.4. Microscale weathering profiles

To examine the impacts of the buried remains on mineral weathering processes in a micro-scale context, the weathering of volcanic glass was assessed by point counting within individual sub-divisions of thin

sections cut perpendicular to the skeletal remains (Fig. 7).

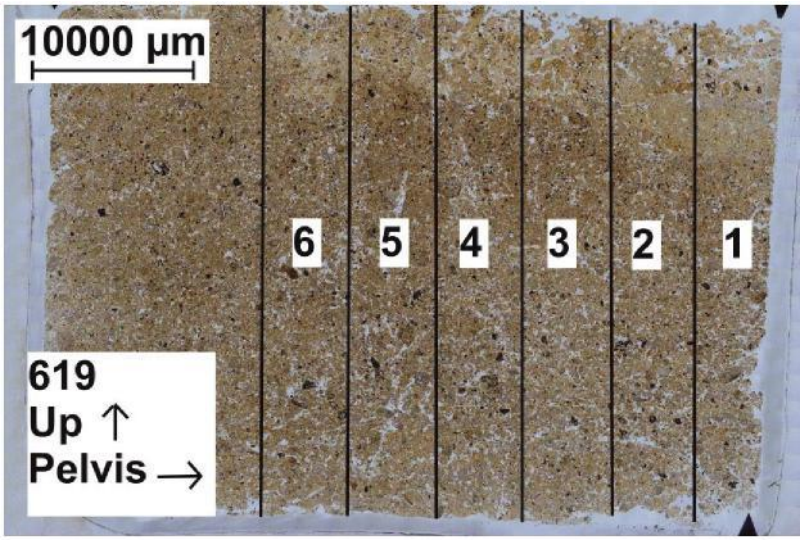

Fig. 7: Section 619 (Grave HSM-A-117, pelvic sample) illustrating the demarcation of sub-divisions at 0.5 cm intervals from the edge of the thin section closer to the skeletal remains. The top of the thin section is at the top of the image and the pelvis was located towards the right of the thin section as shown. [Grayscale image provided]

Statistical evaluation of correlations among the weathering extents reveals a trend with distance from the skeletal remains (Table 4). The trend provides clear evidence of decreasing extent of weathering with increasing distance from the contact with the skeletal remains (s1) up to s5 (Table 4), supporting the interpretations from the tangential thin sections. The break in the trend between s5 and s6 suggests that the latter was influenced by proximity to another source of organic matter (e.g. the coffin). Further studies are needed to determine if the trend of increasing impact on the mineral constituents with increasing proximity to the human remains applies more generally than to just this particular set of grave fills.

Table 4: Two-tailed Pearson's correlation significance test for extent of weathering of volcanic glass in sub-divisions (s1-s6) of thin sections from the skull, pelvic, and foot regions of all seven graves (HSM-A-114 to 120). Sub-division 1 (s1) is closest to the skeletal remains and s6 furthest from the remains (see Fig. 7). (Data from point counting of 79 micro-units in total)

		s1	**s2**	**s3**	**s4**	**s5**	**s6**
s1	Pearson correlation	1	**0.850****	**0.841****	0.601*	0.348	0.676*
	Significance		0.000	0.000	0.014	0.204	0.016
	n	16	16	16	16	15	12
s2	Pearson correlation	**0.850****	1	**0.820****	0.522*	0.201	0.510
	Significance	0.000		0.000	0.038	0.472	0.091
	n	16	16	16	16	15	12
s3	Pearson correlation	**0.841****	**0.820****	1	0.268	0.107	0.530
	Significance	0.000	0.000		0.316	0.703	0.076
	n	16	16	16	16	15	12
s4	Pearson correlation	0.601*	0.522*	0.268	1	0.335	**0.778****
	Significance	0.014	0.038	0.316		0.223	0.003
	n	16	16	16	16	15	12
s5	Pearson correlation	0.348	0.201	0.107	0.335	1	**0.587***
	Significance	0.204	0.472	0.703	0.223		0.045
	n	15	15	15	15	15	12
s6	Pearson correlation	0.676*	0.510	0.530	**0.778****	0.587*	1
	Significance	0.016	0.091	0.076	0.003	0.045	
	n	12	12	12	12	12	12

* Correlation significant at the 0.05 level and ** at the 0.01 level (2-tailed).

3.5. Elemental analysis

Bulk elemental analysis revealed the fills to contain relatively high amounts of organic carbon. Total organic carbon (TOC) contents for the fills from HSM-A-116 ranged from 1.2-3.8% with higher values between 5.1 and 5.9% measured for samples 1z, 13z and A9. TOC contents for the fills from HSM-A-119 were generally higher than those of HSM-A-116, consistent with the higher loam content of the fill, ranging from 3.3-5.5% with higher values of 7.5 and 7.6% observed for the samples from the chest (15y+z) and a dark deposit above top of femur (A1), respectively. During sampling of this grave, an ash deposit was tentatively identified over the chest and could explain the elevated TOC value for 15y+z.

3.6. Organic chemical analysis of sediment lipid extracts

Organic chemical analysis was performed on extracts from the control fills (C2 and C3) and burial samples collected from multiple anatomical locations on the skeletal remains of HSM-A-116 and 119 (Table 1). GC-MS analysis revealed the extractable lipid component of the fills to be dominated by homologous series of *n*-alkanoic acids, ω-hydroxy alkanoic acids, *n*-alkanes, *n*-alkanols, α,ω-diacids and *n*-alkan-2-ones and with the relative abundances of each lipid class generally decreasing in that order. The *n*-alkanoic acids ranged from C_{16}-C_{34} and exhibited distributions with a strong even/odd carbon chain predominance and maxima at C_{24} and C_{26}. The *n*-alkanols ranged from C_{20}-C_{30}, showed an even/odd predominance and maximum at C_{22}. The *n*-alkanes ranged from C_{19}-C_{35} and exhibited distributions with a strong odd/even carbon preference and maximum at *n*-C_{27}. The patterns of *n*-alkanols, *n*-alkanols and *n*-alkanoic acids are characteristic of the epicuticular waxes of vascular plants (Eglinton and Hamilton, 1967) and most likely represent degraded plant matter within the fills. Similar distributions have been observed for other soils (Amblès et al., 1994; Jambu et al., 1991; Jansen et al., 2008) .

The ω-hydroxy alkanoic acids and α,ω-dicarboxylic acids both exhibited a narrow range (C_{20}-C_{28}) of predominantly even chain homologues with distributions dominated by C_{22} and C_{24} members. Terminal oxidation of either *n*-alkanols or *n*-alkanoic acids by soil microorganisms is a potential source of ω-hydroxy alkanoic acids in the grave fills, cf. (Amblès et al., 1994). Similarly, α,ω-dicarboxylic acids could be formed from microbial oxidation of *n*-alkanoic acids or ω-hydroxy alkanoic acids. In the case of the grave fill extracts, the distributions of *n*-alkanols (which contain relatively little C_{24}) and *n*-alkanoic acids (dominated by C_{24} and C_{26}) are at variance with those observed for the ω-hydroxy alkanoic acids and α,ω-dicarboxylic acids suggesting an alternative source for these compounds. Significant amounts of C_{22} and C_{24} ω-hydroxy alkanoic acid and α,ω-dicarboxylic acid moieties occur as polyesters in the biopolymer suberin, which is associated with the exterior surfaces (e.g. bark, roots) of woody plants (Kögel-Knabner, 2002; Van Bergen et al., 1998). Accordingly, the presence these compounds in soil extracts has been proposed to arise via microbial hydrolysis of plant root material (Bull et al., 2000; Van Bergen et al., 1998). It has been suggested that up to half of the organic matter input to soils derives from plant root systems, introduced by dying or sloughing tissue (Hedges and Oades, 1997). Roots were abundant in the grave fills of HSM-A-116 and 119

(e.g. Fig. 3b). Root structures are thought to impact buried human remains via mechanical damage, driving mineral equilibria and the introduction of saprophytic microorganisms as part of the root's natural microbiome (Janaway, 1996; Sagara et al., 2008). While significant variation in the abundances of ω-hydroxy alkanoic acids and α,ω-dicarboxylic acids relative to the other compound classes was observed across the samples, indicative of varying root input, no pattern was observed with regards to the interred remains that could link them with differences in the extent of weathering observed by micromorphological analysis. Instead, the variation in ω-hydroxy alkanoic acids and α,ω-dicarboxylic acids in the grave fills probably reflects the heterogeneous input expected for root-derived material.

The distribution pattern of *n*-alkan-2-ones (C_{21}-C_{35}) exhibited a strong similarity to that of the *n*-alkanes, both exhibiting a clear odd/even carbon chain predominance and maximum at C_{27}. Such *n*-alkan-2-ones are not primary plant products and the similarity of their distributions to those of the *n*-alkanes implies that microbial oxidation of the latter is the source for *n*-alkan-2-ones in the grave fills, cf. (Amblès et al., 1993; Jansen and Nierop, 2009; Van Bergen et al., 1998). Notably, *n*-alkan-2-ones have been identified as primary transformation products of *n*-alkanes in another andosol (volcanic ash soil) (Jansen and Nierop, 2009).

Short chain fatty acids ($<C_{20}$) were present in very low abundance in all of the samples and controls and exhibited little variation. Triacylglycerols, the major lipid components of adipose tissue, contain short chain fatty acids in this range. Thus, no residual signature of the body fat could be detected in these graves. The lack of detectable signatures relating to the body is likely to be due mainly to the permeability of the volcanic sediment to percolating groundwater, facilitating transport of sediment particles and associated organic matter away from the burial. The bacterial markers *iso* and *anteiso* C_{15} and C_{17} fatty acids occurred in low abundance in all samples and other common markers such as bacterial hopanoids were absent. The paucity of bacterial markers is indicative of low levels of bacterial activity within the sediment. Micromorphological analysis has provided evidence of past fungal activity within the sediment from HSM-A-116. Chemical analysis failed to detect corresponding markers for fungal input (such as the fungal sterol ergosterol) indicating that the mineralogical evidence for fungal activity may be more enduring.

Several tricyclic diterpenoids were identified from their mass spectra (as the methyl esters, ME, due to derivatisation) in the extract from beneath the skull (1z) of HSM-A-116 (Fig. 8) but were absent from the controls. These include dehydroabietic acid (ME: $M^{+\cdot}$ 314, 299, 255, <u>239</u>, 185, 173), didehydroabietic acid (abieta-6,8,11,13-tetraenoic acid; ME: $M^{+\cdot}$ 312, 297, 253, <u>237</u>, 197), 7-oxo dehydroabietic acid (ME: $M^{+\cdot}$ 328, 313, 269, <u>253</u>, 187), pimaric acid (ME: $M^{+\cdot}$ 316, 301, 257, 241, 180, <u>121</u>), sandaracopimaric acid (ME: $M^{+\cdot}$ 316, 301, 257, 241, <u>121</u>) and isopimaric acid (ME: $M^{+\cdot}$ 316, 301, 257, <u>241</u>, 187).

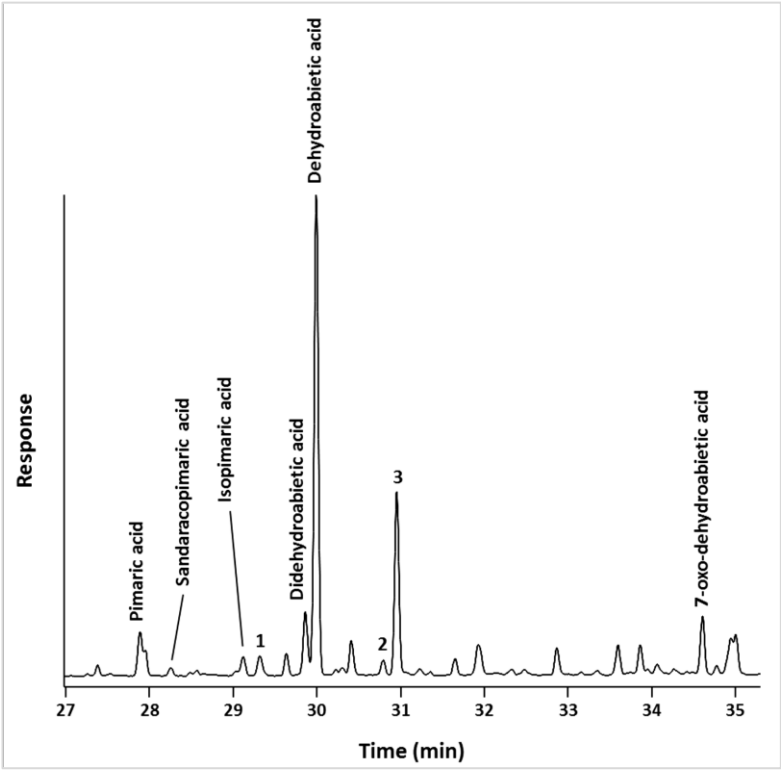

Fig. 8. Partial GC-summed extracted ion mass chromatogram (*m/z* 121+237+239+241+253) for the acid fraction from beneath the skull (1z) of HSM-A-116. Components were detected as their methyl esters (ME). Extracted ions correspond to the base peak ions (underlined in Section 3.6) in their mass spectra. Peaks 1, 2 and 3 represent the trimethylsilyl esters of pimaric acid, didehydroabietic acid and dehydroabietic acid, respectively, resulting from incomplete methylation of those components during derivatisation with trimethylsilyl diazomethane

Dehydroabietic acid, didehydroabietic acid and 7-oxo-dehydroabietic acid are oxidative transformation products of abietic acid which, together with pimaric/isopimaric acids, occur in the fresh resins of the families Coniferae (conifers) (Mills and White, 1994; Simoneit et al., 1986). Dehydroabietic acid (which

occurs only as a minor component in fresh bleed resins) and 7-oxo-dehydroabietic acid are often prevalent in aged conifer resins (Mills and White, 1994; Pollard and Heron, 1996). The abundance of abietic acid, pimarane and isopimarane derivatives in the extract from 1z and lack of detectable phenolic abietanes and totaranes is typical of resins of the Pinaceae (pine family) (Cox et al., 2007; Otto and Wilde, 2001). Within the Pinaceae, pimaranes, such as pimaric acid detected in the extract of 1z, have only been described for *Pinus spp.* (pines), *Picea spp.* (spruce) and *Larix spp.* (larch) (Otto and Wilde, 2001). Of these genera, *Pinus spp.* and *Picea spp.* are the most likely sources of the diterpenoids in the grave, *Larix spp.* resins being distinguished by the labdanoids larixyl acetate (present in significant amount) and larixol (Mills and White, 1994) which were not detected in the extract.

The identification of conifer resin in the grave of HSM-A-116 is supported by pyrolysis-GC analysis performed on small fragments of wood (A3 above thighs and A4 left hip) recovered from this grave which revealed a series of guaiacyl (2-methoxyphenol) monomers deriving from the lignin component of the wood. These included guaiacol, 4-methyl guaiacol, 4-vinyl guaiacol, euginol, vanillin and isoeuginol which were not detected in pyrolysates of the controls. The distribution of guaiacyl moieties and absence of syringyl (2,6-dimethoxyphenol) subunits in the pyrolysate indicates that the wood is of gymnosperm origin (softwood) and is consistent with the products generated from pyrolysis of modern pine wood (data not shown).

The occurrence of abietane and (iso)pimarane diterpenoids and complementary pyrolysis data indicate the presence of wood of the pine family in the grave of HSM-A-116, consistent with the remains of a coffin. At the time of the inhumation, Icelandic woodland primarily comprised birchwood with much lesser amounts of tea-leaved willow, rowan and aspen (Lawson et al., 2007): conifers such as pines that had populated Iceland during the lower and middle Pliocene did not survive beyond the Pleistocene glacial intervals (Rundgren and Ingólfsson, 1999). Accordingly, the conifer wood utilised in the burial of HSM-A-116 must have been either imported, for example from neighbouring Scandinavia, or salvaged driftwood. Driftwood has long played an important part in the history of Iceland (Eggertsson, 1993). The Norse settlement of Iceland in the 9th century led to the destruction of many sensitive birch forests (Lawson et al., 2007) and

without driftwood inhabitation would have been near impossible (Eggertsson, 1993 and references therein). Present day Icelandic driftwood comprises predominantly trees of *Pinus spp.*, *Picea spp.* and *Larix spp.* and originates mainly from the boreal forests of Russia/Siberia; being first transported by rivers draining into the Arctic Ocean, frozen in sea ice and carried by the Transpolar and East Greenland currents to Icelandic shores (Eggertsson, 1993). Hofstaðir is located in northeastern Iceland approx. 45 km from the coast. It is likely that the wood used in the coffin of HSM-A-116 was driftwood originating from such a source.

The pyrolysis profiles of the wood fragments lack signatures from cellulose and hemicellulose, indicating complete degradation of the wood holocelluose. Evidence for the degradation of the wood lignin component comes from the higher levels of short chain monomers (guaiacol, 4-formylguaiacol and 4-acetylguaiacol) than in modern pine. Such evidence of depolymerisation and subsequent oxidation is a feature of degradation by lignin peroxidase, a lignolytic enzyme found exclusively in white rot fungi such as *Phanerochaete chryspospo*rium (Bugg et al., 2011; Geib et al., 2008; Tien, 1987; Tien and Kirk, 1984; Umezawa et al., 1982). Greater proportions of demethoxylated guaiacyl sub units than in modern pine provide further evidence of lignin degradation, attributed to microbial activity (Martínez et al., 2005). The observation, by SEM, of distinct banding of earlywood and latewood cells in of the wood fragments support its identification as gymnosperm. The cellulose-rich secondary cell walls are extensively degraded and the lignin-rich middle lamella are also partly degraded (Fig. 9a). The cellular damage bears a strong resemblance to that caused by white rot (Blanchette et al., 1990), consistent with the presence of fungal spores similar to those the white rot *Phanerochaete chrysosporium* (Rice et al., 2006). Surface analysis by SEM (**Error! Reference source not found.**b) revealed a fungal body of *c.* 100 µm in diameter penetrating the wood at both ends and having numerous hyphae adhering to the wood. The wood cells are heavily damaged and have separated into individual tracheids or bundles of tracheids in the immediate vicinity of the fungal hyphae. The chemical and SEM identification of coffin remains in the burial fully support the micromorphological interpretation of the discontinuity in the weathering ratios between subunits 5 and 6, specifically the proximity of the latter to a coffin (Section 3.3).

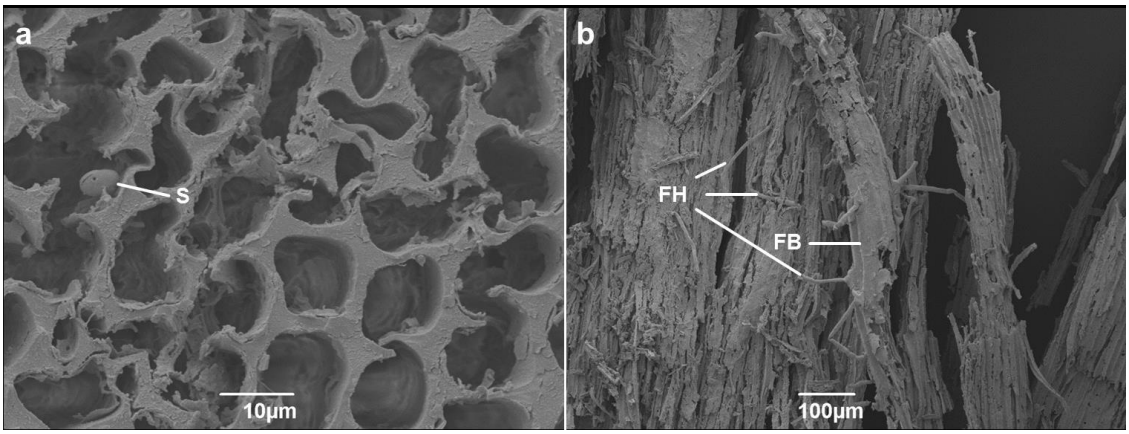

Fig. 9. SEM images of coffin wood sample A3 from grave HSM-A-116 at the Hofstaðir cemetery excavation. Image (a) shows a cross sectional cut of degraded tracheid cells with damage to all cell wall layers and the presence of fungal spores. Image (b) shows a fungal body approximately 100 µm in diameter adhered to the surface of the wood by fungal hyphae which have penetrated in to the wood. Key to abbreviations: fungal spores (S), fungal body (FB), fungal hyphae (FH).

4. Conclusions

Organic chemical analysis performed on two graves (HSM-A-116 and 119) has revealed the extractable lipid components of the grave fills to be dominated by autochthonous components of the soil deriving from plant sources. These sources include leaf waxes and an important contribution from roots. The presence of *n*-alkan-2-ones in the extracts provides evidence of microbial reworking of *n*-alkanes indicating bacterial activity in the soil. No chemical signatures present in the extracts could be attributed to the presence of the interred human remains. By contrast, the results of the micromorphological observation on the seven Hofstaðir graves show significant proxy data for the past presence of organic matter associated with the burial, in particular the evidence of interaction between fungal organisms and readily weathered silicates such as tephra. The evidence from this small selection of graves reflects differences in the weathering extents and patterns of the mineralogical materials between the C1 profile and intra-grave samples, and also the evidence from the materials within the burials compared with the grave control fills and samples adjacent to the remains. Through such knowledge sampling strategies can be tailored to maximise the retrieval of information from the soils and sediments of archaeological burials. Hence, the finding is valuable for archaeological and forensic sciences, in cases of human burials where decomposition is so far

advanced, or the remains have been removed, that no trace of the inhumed corpse is observable with the naked eye.

We argue that the observed fungal-induced weathering effects on tephra may be employed as proxy evidence for fungal activity in the past. The key advantage to this is not only the increase in the period during which the presence of organic matter can be recorded in the archaeological record (albeit via proxy data), but also the highly detailed preservation of the spatial distribution of this data. Potentially, this can enable inferences on the location of an inhumed individual despite a lack of macro-scale visual evidence for a body within a grave. Comparison of thin sections taken tangentially with those taken perpendicular to the skeletal remains, with the aim of identifying proxy evidence for the presence of a body at a small scale within grave cuts, is inconclusive (Table 4). The information obtained would benefit from additional future studies on graves soils within andosols.

Chemical signatures of Pinaceae in HSM-A-116 are indicative of burial in a coffin. Conifers trees did not exist on Iceland at the time of burial so the evidence for a coffin constructed of wood of the pine family indicates either trade in foreign lumber with countries outside Iceland or salvaged driftwood, most likely originating from Russia/Siberia

Acknowledgements

The research has received funding from the European Research Council under the European Community's Seventh Framework Programme (FP7/2007-2013) / ERC grant agreement n°230193 and the NERC (studentship support for APP). We thank the Institute of Archaeology, Iceland (Fornleifastofnun Íslands) for allowing the InterArChive project both access to the site at Hofstaðir and the collection of samples.

References

Amblès, A., Jambu, P., Jacquesy, J.C., Parlanti, E., Secouet, B., 1993. Changes in the ketone portion of lipidic components during the decomposition of plant debris in a hydromorphic forest-podzol. Soil Science 156, 49-56.

Amblès, A., Jambu, P., Parlanti, E., Joffre, J., Riffe, C., 1994. Incorporation of natural monoacids from plant residues into an hydromorphic forest podzol. European Journal of Soil Science 45, 175-182. Doi: 10.1111/j.1365-2389.1994.tb00499.x

Arnalds, Ó., Oskarsson, H., 2007. Icelandic Volcanic Soil Resources, in: Arnalds, Ó., Bartoli, F.,Buurman, P., Oskarsson, H., Stoops, G., Garcia-Rodeja, E. (Eds.), Soils of Volcanic Regions in Europe. Springer, New York, pp.43-50.

Bell, M., Fowler, P.J., Hillson, S.W., 1996. The experimental earthwork project 1960-1990. CBA Research Report, 100. Council for British Archaeology, York.

Bennett, K.D., Simonson, W.D., Peglar, S.M., 1990. Fire and man in post-glacial woodlands of eastern England. Journal of Archaeological Science, 17, 635-642.doi: 10.1016/0305-4403(90)90045-7

Bennett, P.C., Rogers, J.R., Choi, W.J., Hiebert, F.K., 2001. Silicates, silicate weathering, and microbial ecology. Geomicrobiology Journal. 18, 3-19. doi:10.1080/01490450151079734

Blanchette, R.A., Nilsson, T., Daniel, G., Abad, A., 1990. Biological degradation of wood, in: Rowell, R.M., Barbour, R.J. (Eds.), Archaeological Wood Properties, Chemistry, and Preservation. 196th National Meeting of the American Chemical Society, Los Angeles, California, September 25-September 30, 1988, pp. 141-174. American Chemical Society. doi:10.1021/ba-1990-0225.ch006

Bouma, J., Jongerius, A., Schoonderbeek, D., 1979. Calculation of saturated hydraulic conductivity of some pedal clay soils using micromorphometric data. Soil Science Society of America Journal, *43*(2), 261-264.

Brewer, R. 1964. Fabric and Mineral Analysis of Soils. John Wiley and Sons, New York.

Bugg, T.D., Ahmad, M., Hardiman, E.M., Singh, R., 2011. The emerging role for bacteria in lignin degradation and bio-product formation. Current Opinion in Biotechnology, 22, 394-400.

Bull, I.D., Nott, C.J., van Bergen, P.F., Poulton, P.R., Evershed, R.P., 2000. Organic geochemical studies of soils from the Rothamsted classical experiments - VI. The occurrence and source of organic acids in an

experimental grassland soil. Soil Biology & Biochemistry 32, 1367-1376. Doi: 10.1016/S0038-0717(00)00054-7

Canti, M., 2003. Earthworm activity and archaeological stratigraphy: a review of products and processes. Journal of Archaeological Science. 30, 135-148. doi:10.1006/jasc.2001.0770

Carter, D.O., Tibbett, M., 2008. Cadaver Decomposition and Soil: Processes, in: Tibbett, M. Carter, D.O. (Eds.), Soil Analysis in Forensic Taphonomy: Chemical and Biological Effects of Buried Human Remains. CRC Press Taylor & Francis Group: Boca Raton, pp. 29-52.

Cornwall, I.W., 1958. Soils for the Archaeologist. Phoenix House: London.

Courty, M.A., Goldberg, P. and Macphail, R.I. 1989. Soils and Micromorphology in Archaeology. Cambridge University Press Cambridge.

Courty, M. A., Goldberg, P., Macphail, R. I., 1994. Ancient People - Lifestyles and Cultural Patterns, in: Wilding, L., (Ed.), Proceedings of International Soil Science Society. International Soil Science Society, Acapulco, vol. 6a, pp. 250–269.

Cox, R.E., Yamamoto, S., Otto, A., Simoneit, B.R.T., 2007. Oxygenated di- and tricyclic diterpenoids of southern hemisphere conifers. Biochemical Systematics and Ecology 35, 342-362. Doi: 10.1016/j.bse.2006.09.013

Crowther, J., Macphail, R.I., Cruise, G.M., 1996. Short-term, post-burial change in a humic rendzina soil, Overton Down, experimental earthwork, Wiltshire, England. Geoarchaeology. 11, 100-117. doi:10.1002/(SICI)1520-6548(199603)11:2<95::AID-GEA1>3.0.CO;2-4

Delvigne, J., Bisdom, E.B.A., Sleeman, J., Stoops, G., 1979. Olivines, their pseudomorphs and secondary products. Pedologie 29, 247-309.

Delvigne, J.E., 1998. Atlas of Micromorphology of Mineral Alteration and Weathering. The Canadian Mineralogist, Special Publication, no. 3. Mineralogical Association of Canada: Ontario, Canada.

Eggertsson, Ó., 1993. Origin of the driftwood on the coasts of Iceland: a dendrochronological study. Jökull 43, 15-32.

Eglinton, G., Hamilton, R.J., 1967. Leaf epicuticular waxes. Science 156, 1322-1335. doi: 10.1126/science.156.3780.1322

Eswaran, H. (1968). Point-counting analysis as applied to soil micromorphology. Pedologie, *18*(2), 238-252.

Geib, S.M., Filley, T.R., Hatcher, P.G., Hoover, K., Carlson, J.E., Jimenez-Gasco, M.d.M., Nakagawa-Izumi, A., Sleighter, R.L., Tien, M., 2008. Lignin degradation in wood-feeding insects. Proceedings of the National Academy of Sciences United States of America, 105, 12932-12937. doi:10.1073/pnas.0805257105

Gestsdóttir, H. 2014. Osteoarthritis in Iceland. An archaeological study. Háskóli Íslands: Reykjavík.

Gestsdóttir, H. 2015. Hofstaðir 2014. Interim Report. Fornleifastofnun Íslands report no. FS557-910117: Reykjavík.

Grossman, R.B., 1964. Composite thin sections for estimation of clay film volume. Soil Science Society of America Proceedings, 28, 132-133.

Hedges, J.I., Oades, J.M., 1997. Comparative organic geochemistries of soils and marine sediments. Organic Geochemistry 27, 319-361. doi:10.1016/S0146-6380(97)00056-9

Huang, P.M., 2011. Soil Phyical-Chemical-Biological Interfacial Interactions: An Overview, in: Huang, Q., P.M. Huang, and Violante, A. (Eds.), Soil Mineral-Microbe-Organic Interactions: Theories and Applications. Springer: Berlin, pp. 3-38.

Isaksen, O., Gestsdóttir, H. 2012. Fornleifarannsókn á kirkjugarði á Hofstöðum í Mývatnssveit sumarið 2011. (Framvinduskrýrsla). Fornleifastofnun Íslands report no. FS485-910114: Reykjavík.

IUSS Working Group WRB, 2006. World reference base for soil resources 2006. World Soil Resources Reports, no. 103. FAO, Rome. P70. doi:10.1017/S0014479706394902

Jambu, P., Amblès, A., Dinel, H., Secouet, B., 1991. Incorporation of natural hydrocarbons from plant residues into an hydromorphic humic podzol following afforestation and fertilization. Journal of Soil Science 42, 629-636. doi:10.1111/j.1365-2389.1991.tb00109.x

Janaway, R.C., 1996. The decay of buried human remains and their associated materials, in: Hunter, J., Roberts, C., Martin, A. (Eds.), Studies in Crime: An Introduction to Forensic Archaeology, pp. 58-85.

Jansen, B., Haussmann, N.S., Tonneijck, F.H., Verstraten, J.M., de Voogt, P., 2008. Characteristic straight-chain lipid ratios as a quick method to assess past forest-páramo transitions in the Ecuadorian Andes. Palaeogeography Palaeoclimatology Palaeoecology 262, 129-139. doi:10.1016/j.palaeo.2008.02.007

Jansen, B., Nierop, K.G.J., 2009. Methyl ketones in high altitude Ecuadorian andosols confirm excellent conservation of plant-specific *n*-alkane patterns. Organic Geochemistry 40, 61-69.

Jongerius, A., Schoonderbeek, D., and Jager, A., 1972. The application of the Quantimet 720 in soil micromorphometry. *The Microscope*, 20, 243-254.

Jongerius, A., 1974. Recent developments in soil micromorphometry, in: Rutherford, G.K. (Ed.), Soil Microscopy, Proc. 4th Int. Soil Micromorphology Working Group, The Limestone Press Kingston, Canada, pp.67-83.

Jongmans, A.G., Van Breeman, N., Lundstrom, U., Van Hees, P.A.W., Finlay, R.D., Srinivasan, M., Unestam, T., Giesler, R., Melkerund, P.A.,Olsson, M., 1997. Rock-eating fungi. Nature. 389, 682-683. doi:10.1038/39493

Kögel-Knabner, I., 2002. The macromolecular organic composition of plant and microbial residues as inputs to soil organic matter. Soil Biology & Biochemistry 34, 139-162.

Kubiëna, W.L., 1938. Micropedology. Collegiate Press: Ames, Iowa.

Kuhn, P., Aguilar, J., Miedema, R., 2010. Textural Pedofeatures and Related Horizons, in: Stoops, G., Marcelino, V., Mees, F. (Eds.), Interpretation of Micromorphological Features in Soils and Regoliths.

Elsevier, Amsterdam, pp. 217-250.

Lawson, I.T., Gathorne-Hardy, F.J., Church, M.J., Newton, A.J., Edwards, K.J., Dugmore, A.J., Einarsson, Á., 2007. Environmental impacts of the Norse settlement: Palaeoenvironmental data from Mývatnssveit, northern Iceland. Boreas 36, 1-19.

Lucas, G. 2009. Hofstaðir. Excavations of a Viking age feasting hall in north-eastern Iceland. Institute of Archaeology Monograph Series-I: Reykjavík.

Macphail, R.I. and Cruise, J. 2001. The soil micromorphologist as team player: a multianalytical approach to the study of European microstratigraphy, in: Goldberg, P., Holliday, V.T., Ferring, C.R. (Eds.), Earth Sciences and Archaeology. Kluwer Academic/Plenum Publishers: New York, pp. 241-267.

Marcelino, V., Cnudde, V., Vansteelandt, S., and Carò, F. (2007). An evaluation of 2D-image analysis techniques for measuring soil microporosity. European Journal of Soil Science, 58(1), 133-140.

Martínez, A.T., Speranza, M., Ruiz-Dueñas, F.J., Ferreira, P., Camarero, S., Guillén, F., Martínez, M.J., Gutiérrez, A., del Río, J.C., 2005. Biodegradation of lignocellulosics: microbial, chemical, and enzymatic aspects of the fungal attack of lignin. International microbiology: the official journal of the Spanish Society for Microbiology, 8, 195.

Matthews, W., French, C.A.I., Lawrence, T., Cutler, D.F., Jones, M.K., 1997. Microstratigraphic traces of site formation processes and human activities. World Archaeology. 29, 281-308. doi:10.1080/00438243.1997.9980378

McKeague, J.A., Guertin, R.K., Valentine, K.W.G., Belisle, J., Bourbeau, G.A., Howell, A., Michalyna, W., Hopkins, L., Page, F., Bresson, L.M., 1980. Estimating illuvial clay in soils by micromorphology. Soil Science, 129, 386-388.

McLoughlin, N., Furnes, H., Banerjee, N.R., Staudigel, H., Muehlenbachs, K., de Wit, M., Van Kranendonk, M.J., 2008. Micro-bioerosion in volcanic glass: extending the ichnofossil record to Archaean basaltic crust, in: Wisshak, M., Tapanila, L. (Eds.), Current Developments in Bioerosion. Springer: Berlin, pp. 371-396.

doi:10.1007/978-3-540-77598-0-19

Miedema, R., 2002. Alfisols, in: Lal, R. (Ed.), Encyclopedia of Soil Science. Marcel Dekker Inc.: New York, pp. 45-49.

Miedema, R., Pape, T., Van der Waal, G.J., 1974. A method to impregnate wet soil samples, producing high-quality thin sections. Netherlands Journal of Agricultural Sciences. 22, 37-39.

Mikuláš, R., 2008. Xylic substrates at the fossilisation barrier: oak trunks (*Quercus sp.*) in the Holocene sediments of the Labe River, Czech Republic, in: Wisshak, M., Tapanila, L. (Eds.), Current Developments in Bioerosion: Erlangen Earth Conference Series. Springer: Berlin, pp. 415-430.

Mills, J.S., White, R., 1994. The Organic Chemistry of Museum Objects, 2nd edition. Butterworth-Heinemann, Oxford.

Murphy, C.P., 1983. Point counting pores and illuvial clay in thin section. Geoderma 31, 133–150. doi:10.1016/0016-7061(83)90004-6

Murphy, C. P., Kemp, R. A., 1984. The over-estimation of clay and the under-estimation of pores in soil thin sections. Journal of Soil Science. 35, 481-495. doi:10.1111/j.1365-2389.1984.tb00305.x

Otto, A., Wilde, V., 2001. Sesqui-, di-, and triterpenoids as chemosystematic markers in extant conifers - a review. Botanical Review 67, 141-238.

Pagliai, M., 2008. Crusts, Crusting. In Chesworth, W. (Ed.), Encyclopedia of Soil Science. Heidelberg: Springer, pp. 171-179.

Pickering, M.D., Lang, C., Usai, M.-R., Keely, B.J, Brothwell, D.R., 2014. Organic residue analysis of soils. In: Loe, L., Boyle, A., Webb, H. and Score, D. (Eds.) “Given to the ground”: a Viking age mass grave on Ridgeway Hill, Weymouth. Dorset Natural History and Archaeological Society Monograph Series; Vol. 23, Oxbow Books Oxford,. pp. 237-245.

Pollard, C.M., Heron, C., 1996. The chemistry and use of resinous substances, In: Archaeological Chemistry.

RSC Paperbacks, Royal Society of Chemistry, Cambridge, pp. 239-270.

Rice, A.V., Tsuneda, A., Currah, R.S., 2006. In vitro decomposition of Sphagnum by some microfungi resembles white rot of wood. FEMS Microbiology Ecology, 56, 372-382. doi: 10.1111/j.1574-6941.2006.00071.x

Rundgren, M., Ingólfsson, Ó., 1999. Plant survival in Iceland during periods of glaciation? Journal of Biogeography 26, 387-396. doi:10.1046/j.1365-2699.1999.00296.x

Sagara, N., Yamanaka, T., Tibbett, M., 2008. Soil fungi associated with graves and latrines: Towards a forensic mycology, in: Tibbett, M., Carter, D.O. (Eds.), Soil Analysis in Forensic Taphonomy. CRC press, London.

Sayle, K.L., Cook, G.T., Ascough, P.L., Gestsdóttir, H., Hamilton, W.D., McGovern, T.H. 2014. Utilization of $\delta^{13}C$, $\delta^{15}N$, and $\delta^{34}S$ analysis to understand ^{14}C dating anomalies within a late Viking age community in northeast Iceland. Radiocarbon 56, 811-821. doi:10.2458/56.17770

Sayle, K.L., Hamilton, W.D., Cook, G.T., Ascough, P.L., Gestsdóttir, H., McGovern, T.H., 2016. Deciphering diet and monitoring movement: multiple stable isotope analysis of the Viking age settlement at Hofstaðir, Lake Mývatn, Iceland. American Journal of Physical Anthropology 160, 126–136. doi: 10.1002/ajpa.22939

Schiffer, M.B. (1987). Formation Processes of the Archaeological Record. 2nd ed. 1996. University of New Mexico Press Albuquerque.

Simoneit, B.R.T., Grimalt, J.O., Wang, T.G., Cox, R.E., Hatcher, P.G., Nissenbaum, A., 1986. Cyclic terpenoids of contemporary resinous plant detritus and of fossil woods, ambers and coals. Organic Geochemistry 10, 877-889.

Stoops, G., 2003. Guidelines for Analysis and Description of Soil and Regolith Thin-Sections. Soil Science Society of America Madison.

Stoops, G., 2010. Micromorphology as a Tool in Soil and Regolith Studies, in: Stoops, G. Marcelino, V., Mees,

F. (Eds). Interpretation of Micromorphological Features of Soils and Regoliths. Elsevier Amsterdam, pp. 1-13.

Stoops, G., Marcelino, V., and Mees, F., 2010. Interpretation of micromorphological features of soils and regoliths. Elsevier Amsterdam.

Tapanilla, L., 2008. The endolithic guild: an ecological framework for residential cavities in hard substrates, in: Wisshak, M., Tapanila, L. (Eds.), Current Developments in Bioerosion: Erlangen Earth Conference Series. Springer: Berlin, pp. 3-20. doi:10.1007/978-3-540-77598-0-1

Terribile, F., FitzPatrick, E.A., 1995. The application of some image-analysis techniques to recognition of soil micromorphological features. European Journal of Soil Science. 46, 29-45.

Tien, M., 1987. Properties of ligninase from *Phanerochaete chrysosporium* and their possible applications. CRC Critical Reviews in Microbiology, 15, 141-168. doi:10.3109/10408418709104456

Tien, M., Kirk, T. K., 1984. Lignin-degrading enzyme from *Phanerochaete chrysosporium*: purification, characterization, and catalytic properties of a unique H_2O_2-requiring oxygenase. Proceedings of the National Academy of Sciences United States of America, 81, 2280-2284. doi:10.1073/pnas.81.8.2280

Umezawa, T., Nakatsubo, F., Higuchi, T., 1982. Lignin degradation by *Phanerochaete chrysosporium*: Metabolism of a phenolic phenylcoumaran substructure model compound. Archives of Microbiology, 131, 124-128.

Usai, M.-R., Pickering, M.D., Wilson, C.A., Keely, B.J., and Brothwell, D.R., 2014. “Interred with their bones”: soil micromorphology and chemistry in the study of human remains. Antiquity Project Gallery, 88, 339.

Van Bergen, P.F., Nott, C.J., Bull, I.D., Poulton, P.R., Evershed, R.P., 1998. Organic geochemical studies of soils from the Rothamsted classical experiments - IV. Preliminary results from a study of the effect of soil pH on organic matter decay. Organic Geochemistry 29, 1779-1795. doi: 10.1016/S0146-6380(98)00188-0

Vésteinsson, O., Gestsdóttir, H. 2011. Kirkjur og kirkjugarðar, in: Lárusdóttir, B. (ed.) Mannvist. Sýnibók Íslenskra Fornleifa. Opna Reykjavík, pp 72-89.